Supplemental Data Item 2015211

Supplemental Data - DeJong et al., Aug. 2015 GSA Today, Pleistocene relative sea levels in the Chesapeake Bay region and their implications for the next century

Detailed Methods and Data Tables

Drilling and sample collection

The altitude within the study area rarely exceeds 2 m asl, and exposures of surficial deposits and underlying substrate are uncommon, ephemeral, and usually related to land-use practices. Therefore any detailed subsurface exploration requires drilling. Three drilling platforms were used:

Hollow-stem auger system: The cores from the BNWR were collected using a hollow-stem auger continuous sampling system (Figure SD 1A). Sediment cores were collected in 7.6 cm (3 in) diameter plastic liners in an inner core barrel that is straight-pushed inside ~21 cm (8.25 in) diameter augers. These cores were used to collect OSL samples and to provide detailed sedimentologic information about the surface units in and around the BNWR. Sands for OSL were first identified via flight augering and cored inside painted (black) core liners using the hollow-stem coring system. The core liners were carefully extracted from the inner steel core barrel under the tarp, wrapped in black plastic, and placed in a box to ensure the sand was not exposed to light during sampling (Figure SD 2).

Flight Augering: Flight augering (Figure SD 1B) was used for a majority of locations, as this is by far the most cost-effective means of accessing the subsurface. An 11.4 cm (4.5 in) diameter solid-stem auger was drilled into the ground with 1 rotation per auger flight to minimize sediment disturbance and then straight-pulled to the surface for sample collection and analysis. This provided accurate depths to contacts as well as samples for sedimentology and cosmogenic nuclide geochronology (gravel deposits).

Vibracoring: Reconstructing the history of marsh deposits in the Blackwater River valley required drilling from a floating vessel. To accomplish this, we used a hovercraft-mounted, hydraulically powered sonic core (vibracore) drill (Figure SD 1C). This system yielded 6.35 cm (2.5 in) diameter continuous core drilled in 1.52 m (5 ft) sections. The vibracore system was used to collect all samples for sedimentology and radiocarbon geochronology of the Holocene stratigraphy in the Blackwater River valley as well as 2 OSL samples (USU-265, USU-266) directly underlying this stratigraphy.

All drilling locations used in establishing stratigraphic control for this study are indicated in Figure SD 3. Locations with associated geochronology data are labeled and keyed to Tables SD 1-3.

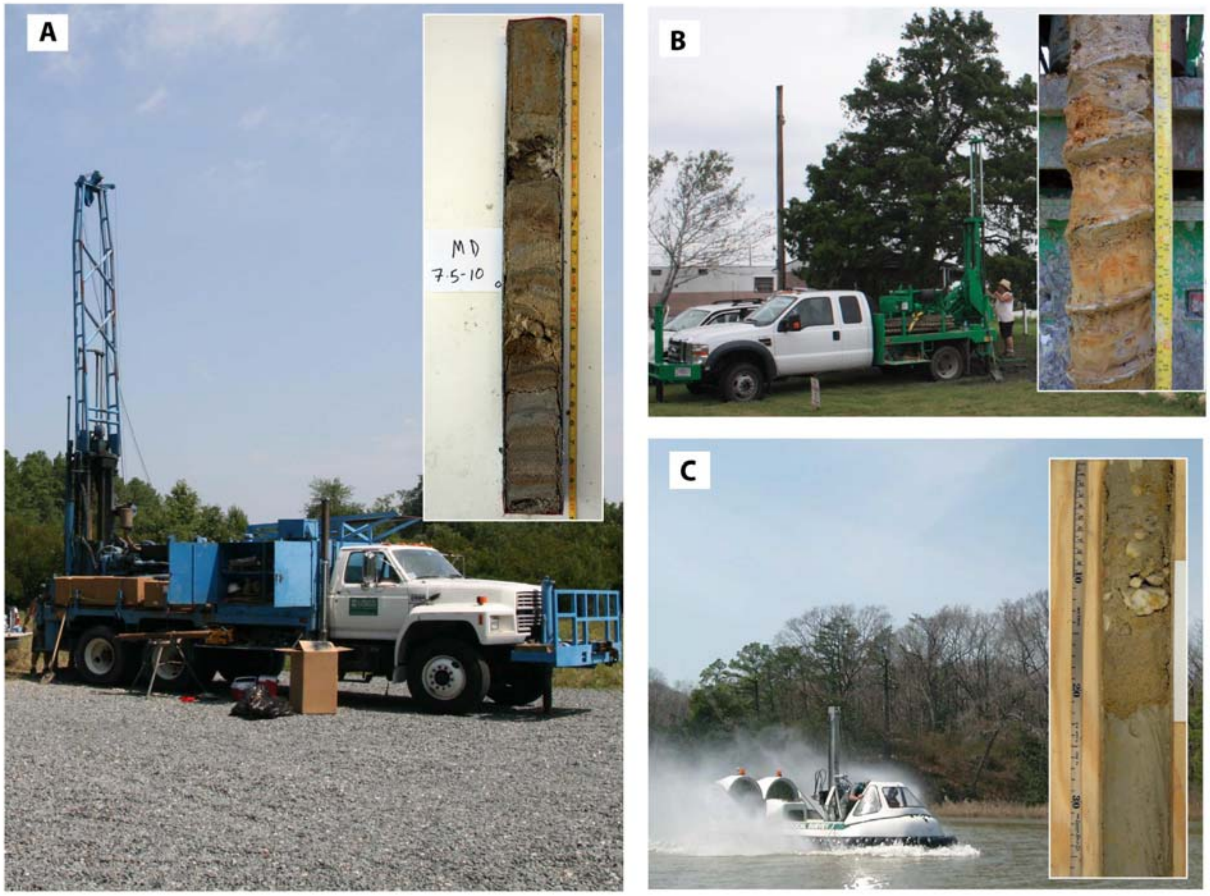

Figure SD 1. *The three platforms used for drilling the BNWR substrate and examples of sediments retrieved from these methods: A) Truck-mounted hollow-stem auger system; B) truck-mounted solid-stem auger system; C) hovercraft-mounted vibracore system.*

Figure SD 2. *OSL field sampling setup. Painted core liner is shown inside split inner core barrel. Sediment cores were collected and packaged under the tarp for transport to the laboratory without being exposed to light.*

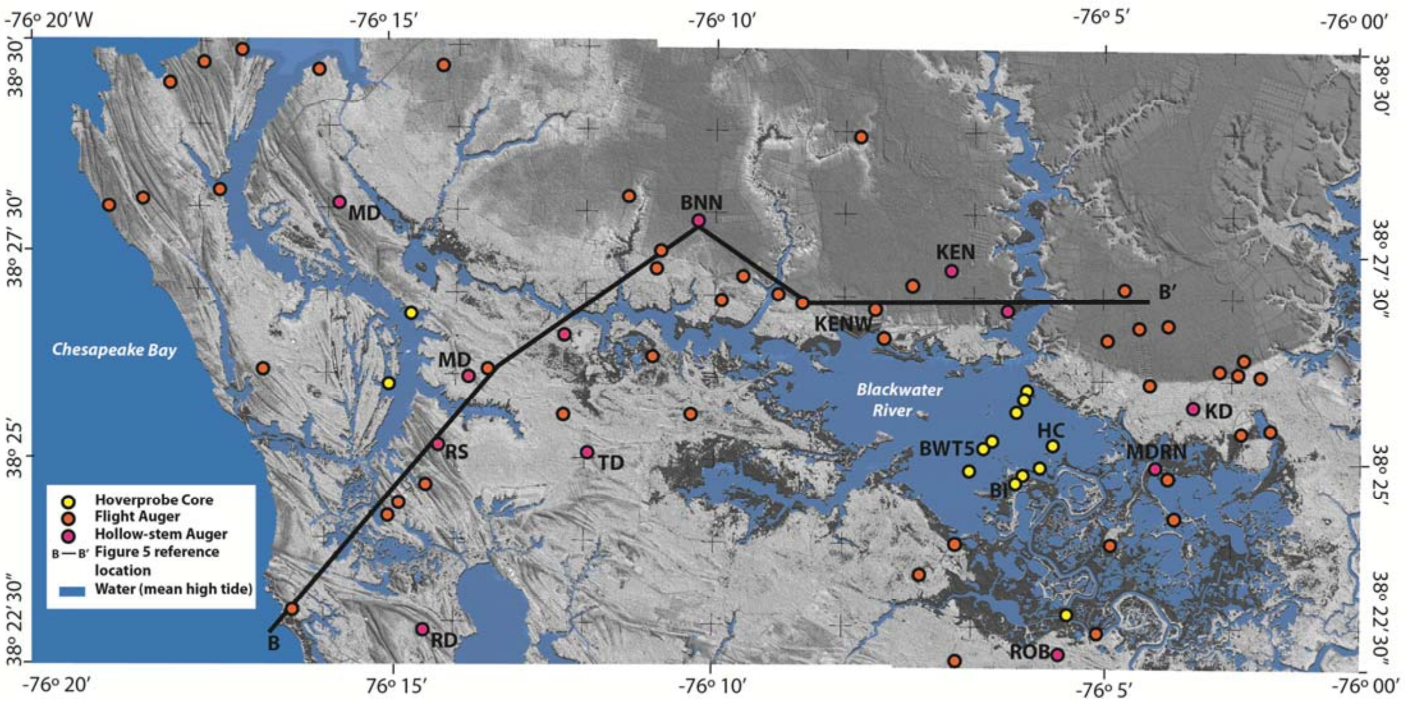

Figure SD 3. *Locations of all boreholes with Figure 3 line of section for reference. Labeled boreholes are keyed to geochronology tables.*

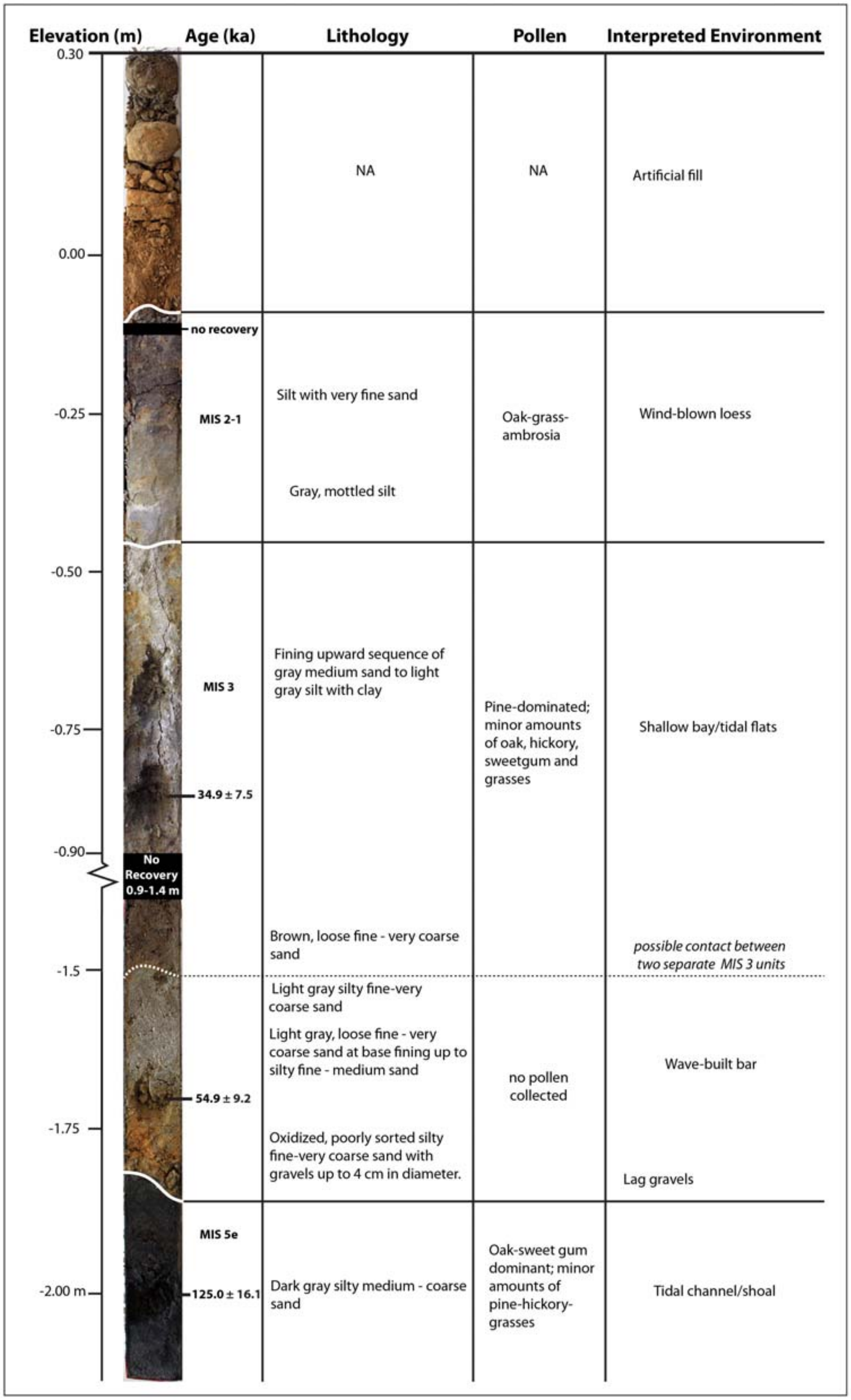

Figure SD 4. *Sediment core from KD (eastern end of Figure 5) showing condensed MIS 3 units truncating MIS 5e unit.*

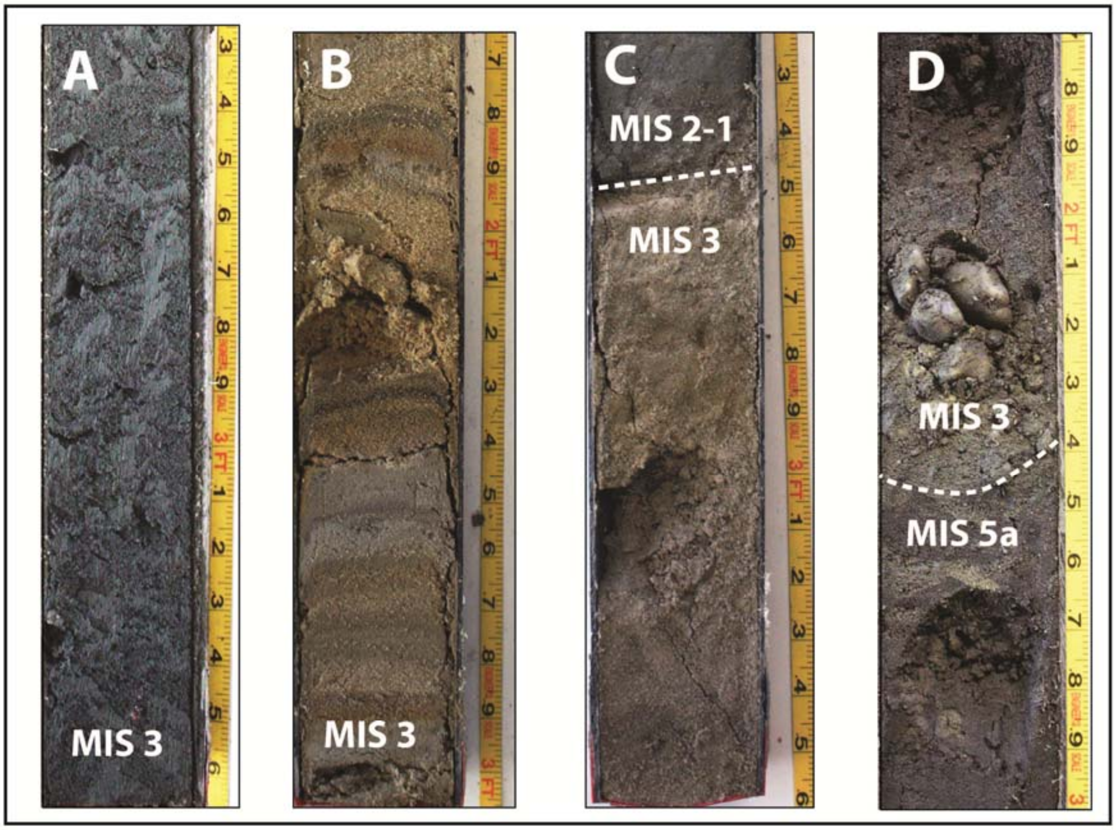

Figure SD 5. *Examples of MIS 3 deposits cored and sampled in this study: A) heavily burrowed estuarine mud and sand bracketed to MIS 3 by underlying sand at the RS location; B) Sand lenses, mud drapes, and heavy mineral laminae from sand bar feature at the MD location; C) massive, shoreline sand from the top of the scarp at the BNN location; D) MIS 3 shoreline sands truncating MIS 5a estuarine sand with a gravelly contact between at the KEN location.*

Cosmogenic radionuclide isochron burial dating

Sample Processing

Sample processing for cosmogenic radionuclide isochron burial dating was completed at the Cosmogenic Radionuclide Laboratory at the University of Vermont according to their standard protocols (Figure SD 6). Individual clasts were sub-sampled from core and auger samples, crushed in a jaw crusher, and ground in a plate grinder to the 90-500 µm fraction. Samples then underwent several acid immersion baths according to Kohl and Nishiizumi (1992) including two 24-hour, 6N HCl baths followed by three 24 hour baths in 0.5% HF, 0.5% HNO_3 solution. The remaining opaque and heavy minerals were removed from the grain size separates (non-clasts) using LST heavy liquid, as these samples tended to be less pure than pulverized clasts. The samples were then dried and tested for purity on an inductively coupled plasma (ICP) optical emission spectrometer. If a sample failed this test, it was treated with one more weak, extended HF-HNO_3 bath.

Once pure, the samples were transferred to the cosmogenic laboratory where they were spiked with ^{9}Be, dissolved completely in concentrated HF, and run through cation and anion columns for isolation of Be and Al. The Be and Al fractions were then precipitated as hydroxides, dried off to form small pellets, and packed into targets with Nb or Ag for measurement at either the Lawrence Livermore National Laboratory (^{10}Be; Rood et al., 2010, 2013) or the Scottish Universities Environmental Research Centre (SUERC) (^{26}Al; Xu et al., 2010, 2014) accelerator mass spectrometers.

DeJong and Bierman were present for Be analyses, and Bierman was present for all Al analyses. Be data were normalized to 07KNSTD3110 with a reported ratio of 2.85×10^{-12} (Nishiizumi et al., 2007). Al data were normalized to the Z92-0222 standard with defined ratio of 4.11×10^{-11} (Xu et al., 2014, 2010).

A blank (Al and Be carrier added with no sample) and an internal standard were processed with each batch. The blanks include the same amount of carrier as samples, so the average measured blank isotopic ratio for all batches in which BNWR samples were processed was subtracted from the measured isotopic ratios of samples (Table SD 2). The long-term average for Be included 4 measurements and yielded an average ^{10}Be/^{9}Be ratio of $7.54 \times 10^{-16} \pm 2.11 \times 10^{-16}$. Five measurements for Al yielded an average ^{26}Al/^{27}Al ratio of $1.60 \times 10^{-15} \pm 9.97 \times 10^{-16}$. The "standard N" of Jull and others (in press) was also run with each batch for inter- and intra-laboratory comparison (Table SD 2).

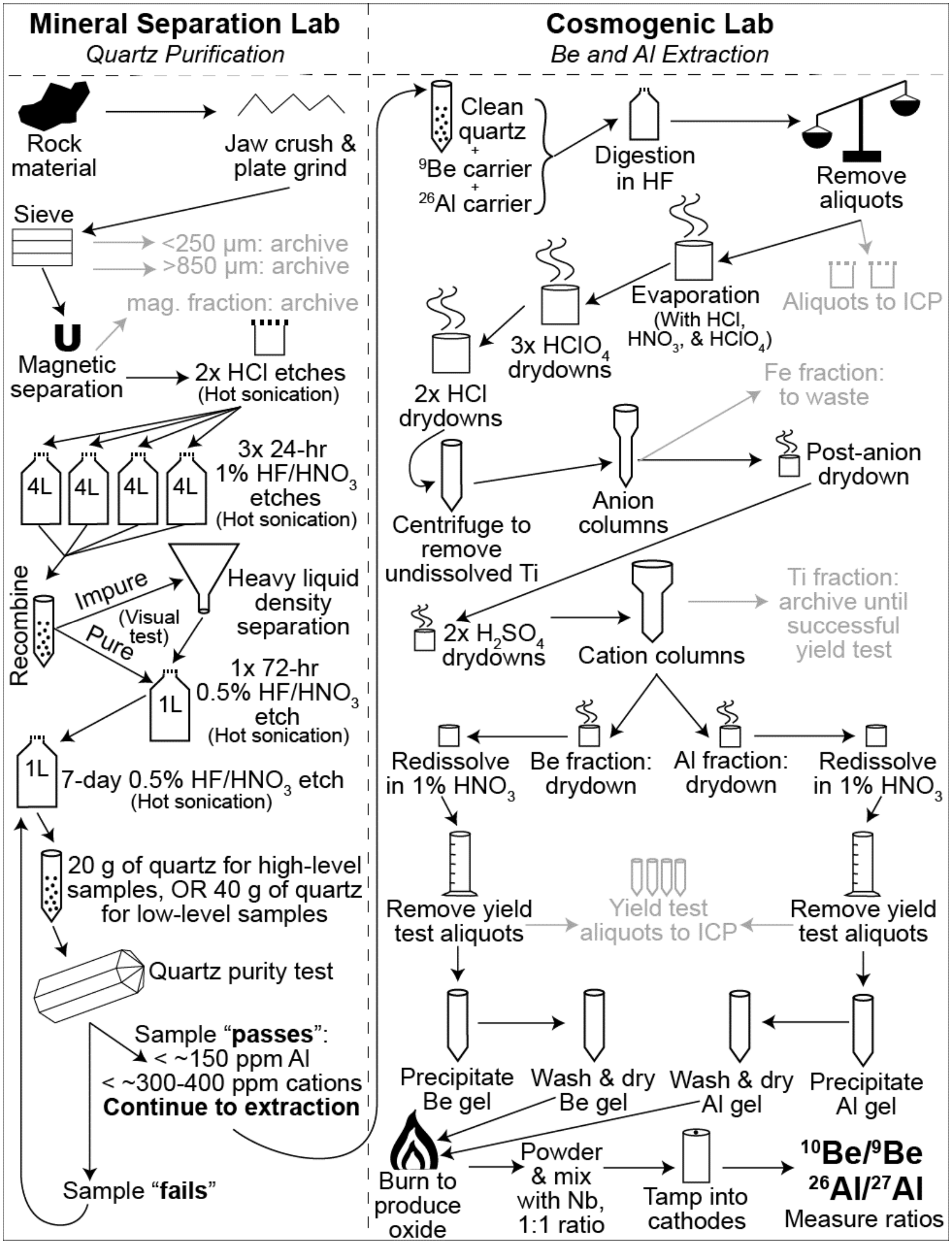

Figure SD 6*. Flow chart showing full processing steps used in the University of Vermont Cosmogenic Radionuclide Laboratory to purify quartz and extract ^{26}Al and ^{10}Be from quartz. Grayed steps include tested (spent) or archived material.*

Data Reduction

The isochron method enables dating of quartz-bearing material with unknown inherited ^{26}Al and ^{10}Be concentrations and unknown burial histories (Balco and Rovey, 2008). Originally developed to date till-paleosol sequences with samples collected from different depths, a variant of this method involves sampling several (≥3) clasts and/or grain size separates from sand fractions that are derived from different settings within the watershed, and thus subject to different exposure histories, but have identical post-burial nuclide production (e.g. they were buried together simultaneously). The ^{26}Al and ^{10}Be concentrations from all clasts and grain size separates form a linear relationship, or an isochron, in ^{26}Al - ^{10}Be space (Figure SD 6). The slope of this isochron depends on the ^{26}Al /^{10}Be production ratio, the ^{26}Al and ^{10}Be decay constants, and on the burial time, but it is independent of the production of nuclides during burial. So if clasts are derived from a wide range of sites with diverse erosion rates, and erosion rates in the watershed are high enough (greater than a few meters per million years) that radioactive decay during transport can be disregarded, the slope of the isochron drawn through ^{26}Al and ^{10}Be concentrations can indicate a burial age for the deposit (Figure SD 7).

The isochron method is appropriate for dating Pleistocene gravels in the BNWR setting. The coarse-grained fluvial deposits that were deposited in discreet stratigraphic horizons derive from a variety of settings within the Susquehanna basin and were buried by sequences of interglacial bay-fill material of variable thickness at unknown rates. Erosion rates quantified for sub-basins in the Susquehanna watershed at a variety of spatial scales indicate rates that are high enough (4-54 m/My; Reuter, 2005) that radioactive decay does not alter the initial ^{26}Al - ^{10}Be ratios of gravels. Additionally, unpublished amino acid racemization dating on several mollusks recovered in bay fill material overlying gravels in BNWR confirm previous findings (Genau et al., 1994) that the age of the channel gravels on the western Delmarva are within the age range datable by the isochron burial dating method (John Wehmiller, personal communication March, 2012).

The measured ^{26}Al and ^{10}Be concentrations ($N_{10,m}$ and $N_{m,}$; atoms g^{-1}) in each individual clast or sand fraction are:

$$N_{10,m} = \frac{P_{10}(0)\Lambda}{\varepsilon} e^{-t_b\lambda_{10}} + N_{10,pb} \tag{1}$$

$$N_{26,m} = \frac{P_{26}(0)\Lambda}{\varepsilon} e^{-t_b\lambda_{26}} + N_{26,pb} \tag{2}$$

where $P_i(0)$ is the surface production rate of the nuclide i (atoms g^{-1} yr^{-1}), Λ is the attenuation length for spallogenic production (generally assumed to be 160 $g{*}cm^{-2}$), ε is the erosion rate ($g{*}cm^{-2}yr^{-1}$) where the clast originated, λ_i is the decay constant for nuclide i, t_b is the duration of burial (yr), and $N_{26,pb}$ and $N_{10,pb}$ are the post-burial ^{26}Al and ^{10}Be concentrations (atoms g^{-1}) in that clast. Because the upstream erosion rate for any particular clast is unknown, ε can be eliminated by solving (1) for Λ/ε and substituting into equation (2). The result is a relationship between the measured ^{26}Al and ^{10}Be concentrations for a set of clasts or grain size fractions of sand:

$$N_{26,m} = \frac{P_{26}(0)}{P_{10}(0)} e^{-(\lambda_{26}-\lambda_{10})t_b} N_{10,m} - \frac{P_{26}(0)}{P_{10}(0)} e^{-(\lambda_{26}-\lambda_{10})t_b} N_{10,pb} + N_{26,pb} \tag{3}$$

Equation (3) is the key to the isochron burial dating method because it yields a linear relationship between measured ^{26}Al and ^{10}Be concentrations from clasts that originated from sites with a range of erosion rates, and the slope of the regression line can determine an age of burial independent of assumptions related to subsurface nuclide production rates or the burial history of the clasts (Figure SD 7).

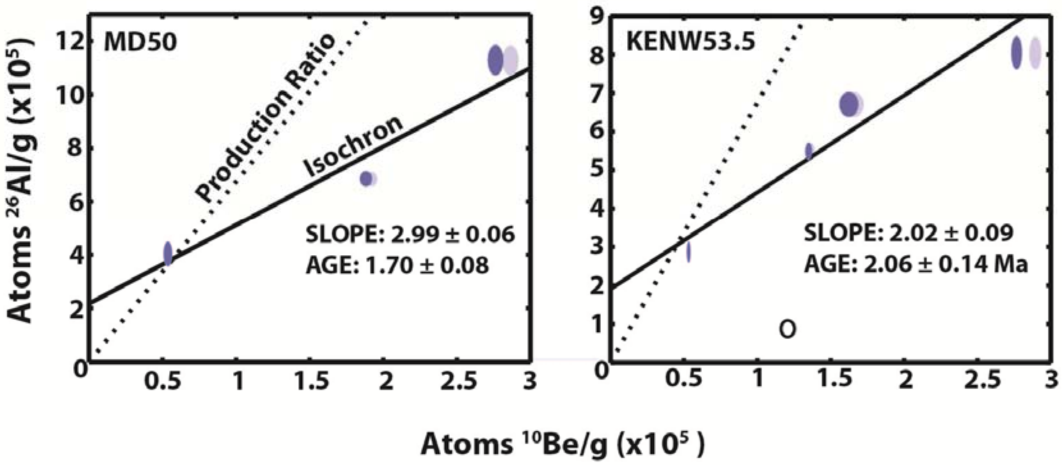

Figure SD 7. *Isochrons produced for gravels at the base of the Pleistocene stratigraphy at the BNWR (2σ ages in Ma). Ellipses indicate 68% confidence regions; light ellipses indicate raw data, dark ellipses indicate linearized data (after Granger, 2014). Errors exclude decay constant uncertainties. The open ellipse in KENW 53.5 indicates a sample that experienced prior burial and was not used in age regression.*

TABLE SD1. Cosmogenic nuclide burial age data

Isochron	Location	Depth in core (m)	Sample ID (UVM ID)	Sample Type	^{10}Be Concentration[a] (atoms/g)	^{26}Al Concentration[b] (atoms/g)	^{26}Al/^{10}Be	Burial Age[c] (Ma)
MD50	38°26'0.33"N 76°13'45.90"W	15.2	B513BL 35	Clast	5.47E+04 ± 2.82E+03	4.03E+05 ± 4.60E+04	7.36 ± 0.92	**1.72 ± 0.08**
			B517BL36	Clast	2.86E+05 ± 5.44E+03	1.13E+06 ± 5.54E+04	3.95 ± 0.21	
			B525BL37A	Sand (500-850 um)	1.92E+05 ± 4.14E+03	6.86E+05 ± 2.72E+04	3.57 ± 0.16	
KENW53.5	38°26'52.97"N 76° 7'26.47"W	16.3	B513BL 18	Clast	5.34E+04 ± 1.24E+03	2.88E+05 ± 2.77E+04	5.39 ± 0.53	**2.06 ± 0.14**
			B513BL 19	Clast	1.37E+05 ± 2.30E+03	5.52E+05 ± 2.19E+04	4.03 ± 0.17	
			B513BL 20	Clast	2.90E+05 ± 4.08E+03	8.09E+05 ± 4.31E+04	2.79 ± 0.15	
			B556BL41	Clast	1.66E+05 ± 6.82E+03	6.74E+05 ± 3.22E+04	4.05 ± 0.25	
			B517BL21	*Clast*	*1.22E+05 ± 3.28E+03*	*7.80E+04 ± 1.58E+04*	*0.64 ± 0.13*	

Data associated with backg round correction

Sample ID (UVM ID)		^{10}Be/^{9}Be	^{26}Al/^{27}Al
B513BLANK		5.76E-16 ± 1.34E-16	1.56E-15 ± 6.38E-16
B517BLANK		5.75E-16 ± 2.52E-16	6.07E-16 ± 4.30E-16
B518BLANK		9.87E-16 ± 1.68E-16	3.13E-15 ± 8.68E-16
B525BLANK		8.77E-16 ± 1.52E-16	1.89E-15 ± 7.71E-16
B521BLANK		NM NM	8.38E-16 ± 4.19E-16
	Average[d]	**7.54E-16 ± 2.11E-16**	**1.60E-15 ± 9.97E-16**

CRONUS Standard[e]

Sample ID (UVM ID)	Quartz (g)	^{9}Be (ug)	^{27}Al (ug)	^{10}Be (atoms/g)	^{26}Al (atoms/g)	^{26}Al/^{10}Be	^{10}Be/^{9}Be	^{26}Al/^{27}Al
B513STAN N	9.57	254.6	3243	2.39E+05 ± 3.73E+03	1.01E+06 ± 3.80E+04	4.25 ± 0.17	1.34E-13 ± 2.10E-15	1.34E-13 ± 5.03E-15
B517STAN N	10.30	253.6	3640	2.26E+05 ± 3.37+03	1.10E+06 ± 5.75E+04	4.85 ± 0.26	1.37E-13 ± 2.05E-15	1.39E-13 ± 7.29E-15
B518STAN N	11.02	253.6	4016	2.21E+05 ± 3.17E+03	1.07E+06± 4.45E+04	4.83 ± 0.21	1.44E-13 ± 2.06E-15	1.31E-13 ± 5.47E-15

[a]Measured at the Lawrence Livermore National Laboratory and normalized to the "07KNSTD" standard with an assumed ratio of 2.85 x 10^{-12}. See Nishiizumi and others (2007)

[b]Measured at the Scottish Universities Environmental Research Centre and normalized to the Z92-0222 standard with defined ratio of 4.11 x 10^{-11}. See Xu and others (2010, 2014)

[c]All ages reported to 2 sigma uncertainly

[d]Long-term average used in background correction

[e]"Standard N" of the CRONUS project. See Jull and others (2013)

Italicized sample experienced prior burial and is not included in age calculation

NM = not measured

Optically Stimulated Luminescence

Sample Processing

All samples were opened and processed at the Utah State University Luminescence Laboratory under dim amber safelight conditions. Sample processing followed standard procedures involving sieving, gravity separation and acid treatments with HCl and HF to isolate the quartz component of a narrow grain-size range. We used the coarsest grained sand fractions possible (250-180 um, except for USU-1211), as suggested for samples deposited subaqueously (Olley et al., 1998). We tested the sensitivity of quartz by ramping stimulating LED's and measuring various components of the OSL signal; the fast component was always >10x higher than the medium and the slow components, indicating that quartz is appropriate for OSL (Stauch et al., 2012). Several samples exhibit high overdispersion values, but the skew is small enough that partial bleaching is not suspected. The purity of the samples was checked by measurement with infra-red stimulation to detect the presence of feldspar. Sample processing procedures followed those outlined in Aitken (1998) and described in Rittenour et al. (2003, 2005).

Data Reduction

The USU and USGS Luminescence Laboratories follow the latest single-aliquot regenerative-dose (SAR) procedures for dating quartz sand (Murray and Wintle, 2000, 2003; Wintle and Murray, 2006). The SAR protocol includes tests for sensitivity correction and brackets the equivalent dose (De) the sample received during burial by irradiating the sample at five different doses (below, at, and above the De, plus a zero dose and a repeated dose to check for recuperation of the signal and sensitivity correction). The resultant data were fit with a saturating exponential curve from which the De was calculated from the Central Age Model (CAM) or the Minimum Age Model (MAM) of Galbraith et al. (1999), depending on the distribution of De results. In cases where the samples have significant positive skew, ages were calculated based on a MAM (e.g. USU-1211, USU-1222, USU-1226). OSL age is reported at 2σ standard error and is calculated by dividing the De (in grays, gy) by the environmental dose rate (gy/ka) that the sample has been exposed to during burial.

Dose-rate calculations were determined by chemical analysis of the U, Th, K and Rb content using ICP-MS and ICP-AES techniques at ALS Chemex, Elko NV and at the USGS Luminescence Laboratory and from conversion factors from Guerin et al. (2011). The contribution of cosmic radiation to the dose rate was calculated using sample depth, elevation, and latitude/longitude following Prescott and Hutton (1994). Dose rates are calculated based on water content, sediment chemistry, and cosmic contribution (Aitken, 1998).

TABLE SD2. Optically stimulated luminescence ages produced for the BNWR stratigraphy

Sample ID (core depth in meters)	Location	% Water content[a]	K (%)[b]	U (ppm)[b]	Th (ppm)[b]	Cosmic dose (Gy/ka)[c]	Total Dose Rate (Gy/ka)	Equivalent Dose (Gy)	n[d]	Scatter[e]	Age[f] (ka)	Correlation[h]	Description
BELOW SCARP													
Tubman (TD)													
USU-1201 (2.59-2.62)	38°25'5.32"N, 76°11'55.96"W	20 (42)	0.51 ± 0.02	1.60 ± 0.08	6.50 ± 0.33	0.15 ± 0.01	1.19 ± 0.16	36.2 ± 5.56	22 (38)	44.3	**30.4 ± 3.4**	MIS 2	Basin rim
USU-1202 (2.83-2.87)		13 (36)	0.50 ± 0.02	0.90 ± 0.05	3.00 ± 0.15	0.14 ± 0.01	0.88 ± 0.12	25.9 ± 4.88	14 (20)	46.9	**29.4 ± 3.5**	MIS 2	Basin rim
USU-1203 (3.35-3.38)		21 (34)	0.60 ± 0.02	0.40 ± 0.10	1.30 ± 0.20	0.14 ± 0.02	0.72 ± 0.10	66.6 ± 7.34	21 (35)	22.6	**92.5 ± 14.2**	MIS 5a/c	Estuarine sand
Russel Swamp (RS)													
USU-1204 (4.39-4.42)	38°25'10.21"N,	21 (28)	0.65 ± 0.02	0.70 ± 0.08	2.40 ± 0.22	0.12 ± 0.01	0.88 ± 0.12	51.7 ± 9.53	24 (38)	41.2	**58.7 ± 12.4**	MIS 3	Base of bar sand
USU-1205 (8.56-8.59)	76°14'14.48"W	*16 (27)*	*0.63 ± 0.02*	*1.10 ± 0.06*	*2.60 ± 0.13*	*0.07 ± 0.01*	*0.97 ± 0.04*	*39.5 ± 3.79*	*12 (27)*	*55.8*	***40.7 ± 4.2[i]***	*MIS 3*	*Base of middle unit*
USU-1206 (8.90-8.93)		18 (40)	0.46 ± 0.01	0.40 ± 0.02	1.10 ± 0.06	0.07 ± 0.01	0.59 ± 0.03	41.4 ± 7.29	20 (24)	60.8	**70.2 ± 12.8**	MIS 5a	Top lower unit
Moneystump (MD)													
USU-1207 (2.50-2.53)	38°26'0.33"N,	14 (26)	0.59 ± 0.02	0.9 ± 0.05	3.45 ± 0.17	0.15 ± 0.01	1.04 ± 0.07	26.9 ± 4.57	12 (20)	44.0	**25.8 ± 4.7**	MIS 2	Basin rim
USU-1208 (2.77-2.80)	76°13'45.90"W	9 (27)	0.38 ± 0.1	0.7 ± 0.04	1.60 ± 0.08	0.15 ± 0.01	0.65 ± 0.08	40.1 ± 5.68	23 (42)	28.7	**62.0 ± 10.8**	Early MIS 3	Bar sand
Parsons (PD)													
USU-1209 (2.68-2.71)	38°28'5.60"N,	10 (36)	0.96 ± 0.03	1.40 ± 0.07	4.90 ± 0.25	0.15 ± 0.01	1.04 ± 0.14	46.3 ± 6.63	20 (43)	27.4	**44.7 ± 7.9**	MIS 3	Top bar sand
USU-1210 (4.42-4.36)	76°15'46.91"W	21 (38)	0.63 ± 0.03	1.10 ± 0.06	2.35 ± 0.12	0.12 ± 0.01	0.94 ± 0.06	42.8 ± 5.56	14 (20)	34.2	**45.5 ± 6.5**	MIS 3	Bottom bar sand
Reber (RD)													
USU-1211 (1.46-1.50)	38°22'56.65"N, 76°14'27.74"W	15 (27)	1.26 ± 0.03	2.8 ± 0.20	10.1 ± 0.90	0.17 ± 0.02	2.33 ± 0.38	83.92 ± 12.38	18 (60)*	18.7	**36.0 ± 6.8**	Late MIS 3	Top bar sand
USU-1212 (2.47-2.50)		18 (27)	0.79 ± 0.04	1.65 ± 0.09	6.20 ± 0.31	0.15 ± 0.01	1.52 ± 0.10	57.6 ± 8.87	9 (15)	25.9	**37.9 ± 6.4**	Late MIS 3	Bottom bar sand
USU-1213 (8.66-8.67)		17 (26)	0.54 ± 0.01	1.1 ± 0.10	1.70 ± 0.20	0.08 ± 0.01	0.81 ± 0.12	36.27 ± 7.81	19 (43)	40.4	**44.8 ± 10.9**	MIS 3	Estuarine sand
Robbins (ROB)													
USU-1221 (280-2.83)	38°22'45.64"N, 76° 4'35.72"W	14 (25)	0.51 ± 0.02	1.30 ± 0.07	3.65 ± 0.18	0.15 ± 0.01	0.97 ± 0.14	66.7 ± 12.7	20 (37)	37.2	**68.7 ± 15.2**	MIS 5a/3	Bar sand
Maple Dam Road (MDRN)													
USU-1215 (1.65-1.68)	38°25'0.24"N,	14 (19)	0.32 ± 0.01	0.5 ± 0.03	1.5 ± 0.08	0.17 ± 0.01	0.65 ± 0.04	24.2 ± 3.42	11 (15)	24.9	**37.4 ± 5.6**	Late MIS 3	Bar sand
USU-1216 (2.04-2.07)	76° 3'14.22"W	17 (22)	0.35 ± 0.01	0.2 ± 0.10	0.60 ± 0.20	0.16 ± 0.02	0.50 ± 0.08	27.6 ± 2.81	20 (29)	15.3	**55.1 ± 8.6**	MIS 3	Bar sand
Kuehnle (KD)													
USU-1218 (1.13-1.16)	38°25'41.57"N, 76° 2'41.53"W	10 (34)	0.20 ± 0.1	0.6 ± 0.03	2.15 ± 0.11	0.18 ± 0.01	0.58 ± 0.04	20.2 ± 4.04	6 (10)	26.7	**34.9 ± 7.5**	Late MIS 3	Bar sand
USU-1219 (1.98-2.01)		14 (24)	0.51 ± 0.01	0.80 ± 0.10	2.20 ± 0.20	0.16 ± 0.02	0.84 ± 0.10	45.82 ± 6.24	21 (50)	25.7	**54.9 ± 9.2**	MIS 3	Bar sand
USU-1220 (2.32-2.35)		20 (28)	0.42 ± 0.01	1.2 ± 0.06	2.4 ± 0.12	0.15 ± 0.01	0.88 ± 0.05	110 ± 12.5	15 (24)	51.5	**125.0 ± 16.1**	MIS 5e	Estuarine sand
Harpers C (HC)													
USU-266 (4.29-4.31)	38°24'54.63"N,	27.3[g]	0.28±0.01	0.6±0.1	3.2±0.3	0.12±0.01	0.65 ± 0.06	27.9 ± 1.9	25 (34)	12.7	**43.2 ± 5.9**	MIS 3	Estuarine sand
USU-265 (4.59-5.61)	76° 4'57.31"W	27.3[g]	0.28±0.01	0.6±0.1	2.7±0.2	0.12±0.01	0.61 ± 0.05	28.3 ± 2.5	25 (32)	17.1	**46.1 ± 6.8**	MIS 3	Estuarine sand
ABOVE SCARP													
Kentuck (KEN)													
USU-1222 (1.92-1.95)	38°27'18.03"N, 76° 6'19.98"W	14 (25)	0.27 ± 0.01	0.90 ± 0.10	2.7 ± 0.20	0.16 ± 0.02	0.70 ± 0.08	28.4 ± 5.38	21 (44)*	22.6	**40.5 ± 8.7**	MIS 3	Shoreline sand
USU-1228 (3.22-3.23)		15 (34)	0.73 ± 0.02	1.90 ± 0.10	5.3 ± 0.27	0.14 ± 0.01	1.40 ± 0.09	68.6 ± 8.92	22 (35)	30.8	**49.0 ± 7.0**	MIS 3	Shoreline sand
USU-1223 (3.29-3.32)		15 (34)	0.89 ± 0.03	2.35 ± 0.12	6.45 ± 0.32	0.14 ± 0.01	1.67 ± 0.11	77.7 ± 6.39	11 (20)	32.8	**46.5 ± 5.0**	MIS 3	Shoreline sand
USU-1224 (5.43-5.46)		18 (27)	0.43 ± 0.01	0.80 ± 0.04	2.0 ± 0.10	0.10 ± 0.01	0.74 ± 0.05	38.9 ± 5.52	9 (10)	11.7	**52.6 ± 8.3**	MIS 3	Base transgression
USU-1225 (5.70-5.73)		20 (28)	0.5 ± 0.10	1.0 ± 0.10	2.7 ± 0.20	0.10 ± 0.01	0.89 ± 0.14	64.0 ± 9.97	24 (52)	30.7	**75.5 ± 14.3**	MIS 5a	Estuarine sand
Buttons Neck (BNN)													
USU-1226 (1.22-1.25)	38°27'52.42"N,	7 (25)	0.24 ± 0.01	0.50 ± 0.10	1.8 ± 0.20	0.18 ± 0.02	0.54 ± 0.12	26.93 ± 3.04	35 (46)*	16.4	**49.8 ± 8.8**	MIS 3	Shoreline sand
USU-1227 (2.35-2.38)	76°10'20.37"W	15 (51)	0.29 ± 0.01	0.83 ± 0.04	2.3 ± 0.12	0.15 ± 0.01	0.64 ± 0.07	33.4 ± 3.34	17 (26)	53.3	**52.3 ± 6.3**	MIS 3	Base transgression

[a]In situ moisture content, with figures in parentheses indicating saturation values (in weight %). Ages calculated using approximately 70% of saturation values.

[b]Analyses obtained using inductively coupled plasma mass spectrometry (ICP-MS). All errors were obtained with calibration standards (i.e. K% error = 3%, U and Th ppm error = 5%).

[c]Cosmic doses and attenuation with depth were calculated using the methods of Prescott and Hutton (1994). See text for details.

[d]Number of replicated equivalent dose (De) estimates used to calculate the equivalent dose. Figures in parentheses indicate total number of measurements included in calculating the equivalent dose and age using the central age model (CAM), while the * represents the minimum age model (MAM).

[e]Defined as "over-dispersion" of the De values. Obtained by taking the average over the standard deviation. Values >20% are considered to be poorly bleached, mixed, or bioturbated sediments.

[f]Dose rate and age for fine-grained 250-180 micron sized quartz. Exponential + linear fit used on equivalent doses; errors to two sigma; ages and errors rounded.

[g]70% of average field capacity moisture content from other samples used for dose-rate calculation

[h]Interpreted MIS correlations based on highest sea level within 2-sigma sample error range based on proxies indicated in Figure 3 of manuscript

[i]Further work is in progress on this sample to identify stratigraphic reversal between this sample and the sample above

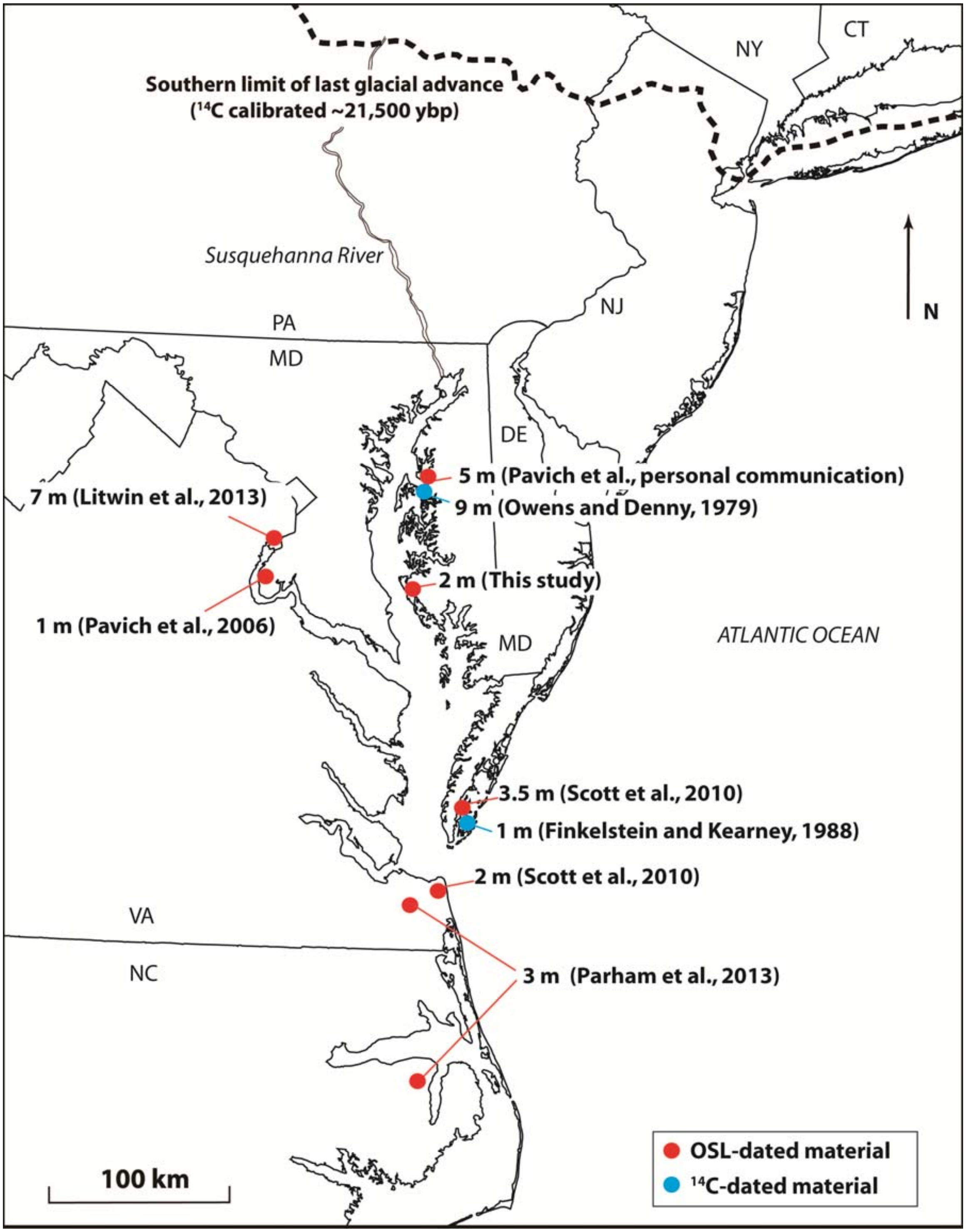

Figure SD 8. *Variability in surface elevations of MIS 3 deposits dated using both OSL and ^{14}C dating. To the knowledge of the authors, no emerged MIS 3 units have been dated and reported in the literature north or south of this region.*

TABLE SD3. Radiocarbon ages produced for the Holocene stratigraphy of the BNWR

USGS ID	Core	Location	Elevation (m)	^{14}C AGE[a]			Calibrated age (yBP)[b]	Description
WW6532	Barbadoes Island (BI)	38°24'45.98"N 76° 5'16.85"W	-3.7	---	---	---	Modern	Plant material; base of peat
WW6533			-3.8	863	±	43	691-907	Plant material; top of silt below peat
WW6535			-7.8	1584	±	35	1400-1550	Plant material in silt
WW6536			-8.0	2087	±	37	1950-2149	Plant material in silt
WW6537			-8.3	1921	±	36	1740-1949	Plant material in silt
WW6539	BW Transect 5 (BWT5)	38°25'12.60"N 76° 5'49.78"W	-3.9	---	---	---	Modern	Plant material; base of peat
WW6540[c]			-8.4	129	±	34	8-277	Plant material in silt
WW6541			-8.6	4660	±	40	5310-5572	Plant material in silt

[a]Standard ^{14}C age (yr) using the Libby half life of 5568 years
[b]Calibrated to calendar years before present (1950) using the INTCAL 13 curve (Reimer et al., 2013) in CALIB 7.0 (Stuiver and Reimer, 1993), full 2-sigma range.
Ages were rounded to 102 years and expressed as "ka" for consistency in Figure 5.
[c]Sample assumed to be out of place and drug in during drilling

References cited (Supplementary Data)

Aitken, M.J. 1998: An Introduction to Optical Dating: The dating of Quaternary sediments by the use of photon-stimulated luminescence. New York, Oxford University Press, 267 pp.

Balco, G., and Rovey, C. W., 2008, An isochron method for cosmogenic-nuclide dating of buried soils and sediments: American Journal of Science, v. 308, no. 10, p. 1083-1114.

Finkelstein, K. F., and Kearney, M. S., 1988, Late Pleistocene barrier-island sequence along the southern Delmarva Peninsula: Implications for middle Wisconsin sea levels: Geology, v. 16, p. 41-45.

Galbraith, R.F., Roberts, R.G., Laslett, G.M., Yoshida, H., Oleey, J.M., 1999. Optical dating of single and multiple grains of quartz from Jinmium Rock Shelter, northern Australia: Part I, experimental design and statistical models: Archaeometry, v. 41, p. 339-364.

Genau, R. B., Madsen, J. A., McGeary, S., and Wehmiller, J. F., 1994, Seismic-Reflection Identification of Susquehanna River Paleochannels on the Mid-Atlantic Coastal Plain: Quaternary Research, v. 42, p. 166-174.

Granger, D. E., 2014, Cosmogenic Nuclide Burial Dating in Archaeology and Paleoanthropology: Treatise on Geochemistry, v. 14, p. 81-97.

Guerin, G., Mercier, N., Adamiec, G., 2011. Dose-rate conversion factors: update: Ancient TL, v. 29, p. 5-8.

Jull, A. J. T., Scott, E. M., and Bierman, P., in press, The CRONUS-Earth inter-comparison for cosmogenic isotope analysis: Quaternary Geochronology.

Kohl, C. P., and Nishiizumi, K., 1992, Chemical isolation of quartz for measurement of in-situ-produced cosmogenic nuclides: Geochimica et Cosmochimica Acta, v. 56, p. 3583-3587.

Litwin, R. J., Smoot, J. P., Pavich, M. J., Markewich, H. W., Brook, G., and Durika, N. J., 2013, 100,000-year-long terrestrial record of millennial-scale linkage between eastern North American mid-latitude paleovegetation shifts and Greenland ice-core oxygen isotope trends: Quaternary Research, v. 80, no. 2, p. 291-315.

Mallinson, D., Burdette, K., Mahan, S., and Brook, G., 2008, Optically stimulated luminescence age controls on late Pleistocene and Holocene coastal lithosomes, North Carolina, USA: Quaternary Research, v. 69, no. 1, p. 97-109.

Murray, A.S., Wintle, A.G., 2000. Luminescence dating of quartz using an improved single aliquot regenerative-dose protocol: Radiation Measurements v. 32, p. 57-73.

Murray, A.S., Wintle, A.G., 2003. The single aliquot regenerative dose protocol: potential for improvements in reliability: Radiation Measurements v. 37, p. 377-381.

Nishiizumi, K., Imamura, M., Caffee, M. W., Southon, J. R., Finkel, R. C., and McAninch, J., 2007, Absolute calibration of 10Be AMS standards: Nuclear Instruments and Methods in Physics Research Section B: Beam Interactions with Materials and Atoms, v. 258, no. 2, p. 403-413.

Olley, J. M., Caitcheon, G. G., and Murray, A. S., 1998, The distrubution of apparent dose as determined by optically stimulated luminescence in small aliquots of fluvial quartz: implications for dating young sediments: Quaternary Science Reviews, v. 17, p. 1033-1040.
Owens, J. P., and Denny, C. S., 1979, Upper Cenozoic deposits of the Central Delmarva Peninsula, Maryland and Delaware, USGS Professional Paper 1067-A: Washington, DC, 27 pp.
Parham, P. R., Riggs, S. R., Culver, S. J., Mallinson, D. J., Jack Rink, W., and Burdette, K., 2013, Quaternary coastal lithofacies, sequence development and stratigraphy in a passive margin setting, North Carolina and Virginia, USA: Sedimentology, v. 60, no. 2, p. 503-547.
Pavich, M. J., and Markewich, H. W., 2006, Significance of Kent Island Formation to geomorphic history of the Mid-Atlantic region: Geological Society of America, Abstracts with programs 38, p. 226.
Prescott, J. R., Hutton, J.T., 1994. Cosmic ray contributions to dose rates for luminescence and ESR dating: Radiation Measurements 23, 497-500.
Reimer, P. J., Bard, E., Bayliss, A., Beck, J. W., Blackwell, P. G., Bronk Ramsey, C., Buck, C. E., Cheng, H., Edwards, R. L., Friedrich, M., Grootes, P. M., Guilderson, T. P., Haflidason, H., Hajdas, I., Hatté, C., Heaton, T. J., Hoffmann, D. L., Hogg, A. G., Hughen, K. A., Kaiser, K. F., Kromer, B., Manning, S. W., Niu, M., Reimer, R. W., Richards, D. A., Scott, E. M., Southon, J. R., Staff, R. A., Turney, C. S. M., and van der Plicht, J., 2013, INTCAL13 and marine13 radiocarbon age calibration curves 0–50,000 years CAL BP: Radiocarbon, v. 55, no. 4, p. 1869-1887.
Reuter, J., 2005, Erosion rates and pattern inferred from cosmogenic 10Be in the Susquehanna River Basin. Unpublished Masters thesis, University of Vermont, 160 p.
Rittenour, T.M., Goble, R.J., Blum, M.D., 2003, An Optical Age Chronology of Fluvial Deposits in the Northern Lower Mississippi Valley: Quaternary Science Reviews, v. 22, p. 1105-1110.
Rittenour, T.M., Goble, R.J., Blum, M.D., 2005, Development of an OSL chronology for late Pleistocene channel belts in the lower Mississippi valley: Quaternary Science Reviews, v.24, p.2539-2554.
Rood, D.H., Hall, S., Guilderson, T.P., Finkel, R.C., Brown, T.A., 2010, Challenges and opportunities in high-precision Be-10 measurements at CAMS, Nuclear Instruments and Methods B: Beam Interactions with Materials and Atoms, v. 268, no. 7-8, p. 730-732.
Rood, D.H., Brown, T.A., Finkel, R.C., Guilderson, T.P., 2013, Poisson and non-Poisson uncertainty estimations of $^{10}Be/^{9}Be$ measurements at LLNL–CAMS, Nuclear Instruments and Methods B: Beam Interactions with Materials and Atoms, v. 294, p. 426-429.
Scott, T. W., Swift, D. J. P., Whittecar, G. R., and Brook, G. A., 2010, Glacioisostatic influences on Virginia's late Pleistocene coastal plain deposits: Geomorphology, v. 116, no. 1-2, p. 175-188.
Stauch, G., Ijmker, J., Pötsch, S., Zhao, H., Hilgers, A., Diekmann, B., Dietze, E., Hartmann, K., Opitz, S., Wünnemann, B., and Lehmkuhl, F., 2012, Aeolian

sediments on the north-eastern Tibetan Plateau: Quaternary Science Reviews, v. 57, p. 71-84.
Stuiver, M., and Reimer, P. J., 1993, Extended ^{14}C database and revised CALIB radiocarbon calibration program: Radiocarbon v. 35, p. 215-230.
Wintle, A.G. Murray, A.S., 2006, A review of quartz optically stimulated luminescence characteristics and their relevance in single-aliquot regenerative protocols: Radiation Measurements, v. 41, p. 369-391.
Xu, S., Dougans, A.B., Freeman, S.P.H.T., Schnabel, C., Wilcken, K.M, 2010, Improved ^{10}Be and ^{26}Al-AMS with a 5 MV spectrometer: Nuclear Instruments and Methods in Physics Research B, v. 268, p. 736–738.
Xu, S., Freeman, S.P.H.T., Rood, D.H., Shanks, R.P., 2014, ^{26}Al interferences in accelerator mass spectrometry measurements, Nuclear Instruments and Methods in Physics Research B, v. 333, p. 42-45.